

Parsimonious modeling of hysteretic structural response earthquake engineering



I. Gidaris , A. Taflanidis

University of Notre Dame, Department of Civil Engineering and Geological Sciences

SUMMARY:

Under strong seismic excitations structural systems exhibit hysteretic behavior. This behavior can be accurately evaluated through high-fidelity numerical models, an approach that typically involves a significant computational cost. This study discusses an alternative simulation framework based on parsimonious modeling of the hysteretic behavior using the SIMULINK modeling environment in MATLAB. This parsimonious modeling is established by describing the restoring force for each floor, based on its corresponding drift. Three different models are considered for the restoring force-displacement relationship. A comprehensive approach is discussed for calibration of these models based on information obtained by a high-fidelity structural model. The accuracy and the computational savings of this parsimonious modeling approach are then examined by comparison to the high-fidelity structural model (developed in OpenSees) over an ensemble of ground motion records. The results show the great computational savings established through the parsimonious modeling approach, at the expense of a small only reduction in accuracy.

Keywords: parsimonious model, hysteretic response, piece-wise linear hysteretic model, Masing, SIMULINK

1.INTRODUCTION

Under strong seismic excitations structural systems exhibit hysteretic behavior and evaluation of their time-history response requires development of high-fidelity numerical models that can adequately describe this behavior. A comprehensive approach for this task involves modeling the structural components as one – dimensional finite elements with distributed inelasticity. This high-fidelity modeling approach is associated, though, with a significant computational burden, which makes its implementation challenging. This is particularly true for probabilistic risk assessment applications which require a large number of structural simulations to estimate seismic risk (Taflanidis and Beck, 2009, Spacone et al., 1996a). The current study discusses a parsimonious modeling approach for the hysteretic behavior of nonlinear structures using the versatile SIMULINK modeling environment in MATLAB (Klee, 2007). This parsimonious modeling is established by globally describing the restoring force for each floor, based on its corresponding drift. Three different models will be considered here for the restoring force-displacement relationship, ultimately representing three different types of hysteretic behavior. A comprehensive approach is discussed for calibration of these models based on information obtained from a high-fidelity structural model. The accuracy and the computational savings of this parsimonious modeling approach are then examined by comparison to the high-fidelity structural model over a large ensemble of ground motion records. The results show the great computational savings established through the parsimonious modeling approach, at the expense of a small only reduction in accuracy. They also validate the established approach for calibrating the parsimonious model using information from the high fidelity one.

2.MODELING OF STRUCTURAL RESPONSE

A parsimonious model for the nonlinear, hysteretic structural response is established by modeling the cumulative restoring forces per story (from all structural elements contributing to that force) through a shear-structure model. In this study we will focus on planar structural models. For a n-story structure

let $\mathbf{x}_s \in \mathfrak{R}^n$ denote the vector of displacements for each floor relative to the base, \mathbf{M}_s , and \mathbf{C}_s correspond to the $n \times n$ mass and damping matrices, respectively, $\mathbf{R}_s \in \mathfrak{R}^n$ to the vector of earthquake influence coefficients, \mathbf{F}_r to the vector of restoring forces for each floor and \mathbf{T}_s the drift transformation matrix. The equation of motion is then

$$\mathbf{M}_s \ddot{\mathbf{x}}_s + \mathbf{C}_s \dot{\mathbf{x}}_s + \mathbf{T}_s^T \mathbf{F}_r = -\mathbf{M}_s \mathbf{R}_s \ddot{\mathbf{x}}_g \quad (1.1)$$

where $\ddot{\mathbf{x}}_g \in \mathfrak{R}$ denotes the ground acceleration. The vector of inter-story drifts is then $\boldsymbol{\delta} = \mathbf{T}_s \mathbf{x}_s$. The restoring forces at each story, F_i , are formulated as a nonlinear function of the corresponding drift at each story, δ_i . The mass matrix \mathbf{M}_s is simply the diagonal matrix consisting of these masses, whereas the damping matrix \mathbf{C}_s can be formulated based on some appropriate modeling assumption. A common approach, also assumed in the illustrative example that will be considered later, is to use Rayleigh damping.

3. PARSIMONIOUS MODELING OF HYSTERETIC STRUCTURES

This section will discuss the hysteretic relationship between restoring forces and inter-story drifts (displacements), F - δ . Two different components can be distinguished for developing these models: (i) definition of the backbone curve, describing the behavior due to cyclically increasing deformation and (ii) definition of the rules that describe the hysteretic behavior due to transient loading. Here, two different classes of models will be considered. Both of them can be very efficiently incorporated within the SIMULINK modeling framework that will be discussed in the next section (this is one of the main reasons for choosing them). The first one is a piecewise linear model, and two different hysteretic models will be considered within this class, an ideal elastic-plastic and a peak-oriented one. The second class corresponds to the generalized Masing model, belonging in the greater family of smooth hysteretic models. For both models possible stiffness and strength deterioration characteristics will be addressed. Initially the mathematical formulation for these models will be presented and then their calibration will be analyzed based on information obtained from high-fidelity (distributed inelasticity finite-element) models.

3.1. Piecewise linear hysteretic model

The simplest case for piecewise hysteretic model is the ideal elasto-plastic spring with no strain hardening. The backbone curve is defined by the initial (elastic) stiffness k_i and the maximum force capacity F_u (for asymmetric cases the force capacity can be considered different in the two directions of loading: F_{u+} and F_{u-} , respectively) or equivalently, by the yield displacement δ_y (or for asymmetric cases δ_{y+} and δ_{y-} , respectively). The subscripts + and - will be used herein to denote characteristics in positive and negative directions, respectively. After the yielding displacement δ_y the force attains its maximum value (no strain hardening) but unloading follows the initial incline until the restoring force retains its maximum value in the other direction (hysteresis rule). If reloading starts before that threshold is attained, then the reloading will follow the initial incline till the maximum value is reached. Note that this model is equivalent to the behavior of a linear spring (with stiffness k_i) in series with a Coulomb friction damper (with friction force F_u). The hysteretic behavior of the ideal elasto-plastic spring can be actually modeled through the following convenient relationship

$$F^{j+1} = \text{sat} \left\{ k_i (\delta^{j+1} - \delta^j) + F^j, F_{u+}, F_{u-} \right\} \quad (1.2)$$

where the superscript j is used to denote the response at the j^{th} time instance t^j and $\text{sat}\{f, u, l\}$ is the saturation function with upper and lower limits u and l , respectively

$$\text{sat}\{h, u, l\} = \begin{cases} u & \text{if } h > u \\ h & \text{if } u \leq h \leq l \\ l & \text{if } h < l \end{cases} \quad (1.3)$$

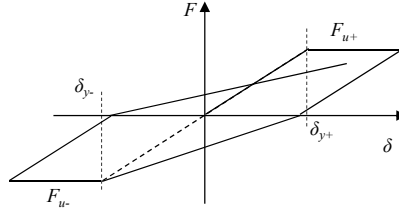


Figure 3.1. Peak-oriented hysteretic model

A modification to the hysteretic rule for this bilinear model is the peak oriented model shown in Figure 3.1. In this case the reloading path targets the previous maximum displacement once the horizontal axis is crossed. If that displacement is not larger than the yielding displacement, then the path targets the yielding displacement. For this model the linear stiffness in (1.2) needs to be modified to

$$k_l^{j+1} = \begin{cases} k_l & \text{if } \delta^j \delta^{j+1} < 0 \text{ (unloading started)} \\ \frac{F_{u+}}{\delta_{mm+} - \delta^j} & \text{if } F^j F^{j+1} < 0 \text{ \& } F^j < 0, \text{ where } \delta_{mm+}(t) = \max\left(\max_{\tau \leq t}(\delta(\tau)), \delta_{y-}\right) \\ \frac{F_{u-}}{\delta_{mm-} - \delta^j} & \text{if } F^j F^{j+1} < 0 \text{ \& } F^j > 0, \text{ where } \delta_{mm-}(t) = \min\left(\min_{\tau \leq t}(\delta(\tau)), -\delta_{y-}\right) \\ k_l^j & \text{else} \end{cases} \quad (1.4)$$

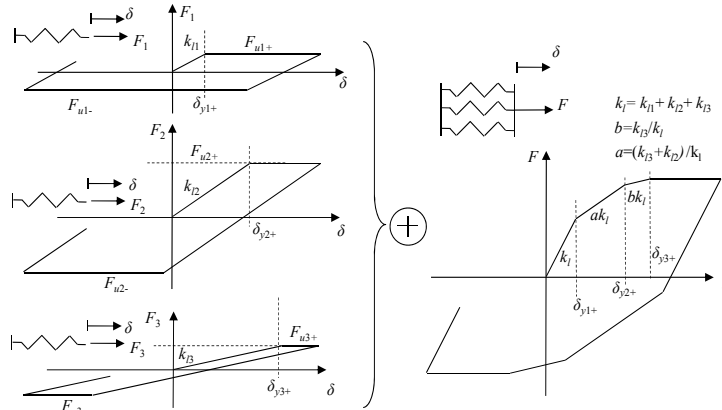


Figure 3.2. Bilinear hysteretic model with strain hardening; individual spring components (left) and resultant restoring force (left)

Combination, now, in parallel connection, of multiple springs leads to more complex piecewise linear restoring force characterization. For example, connection of a linear and an ideal elasto-plastic spring as in Figure 3.2 leads to bilinear restoring force with strain hardening. Such models are calibrated with respect to the characteristics for the backbone curve of the resultant restoring force, which for the example in Figure 3.2 means the linear stiffness k_l , the post yield stiffness ratio a and the yielding displacements δ_{y+} and δ_{y-} . It can be then implemented by combining the simple spring elements, which for the example in Figure 3.2 leads to $k_{l2} = ak_l$, $k_{l1} = (1-a)k_l$, $F_{u1+} = k_{l1}\delta_{y+}$ and $F_{u1-} = k_{l1}\delta_{y-}$.

3.2. Generalized Masing model

The generalized Masing model (Spacone et al., 1996b, Vetter et al., 2012) can be considered as an extension of the distributed element model (Bertero et al., 1978). The latter consists of a collection of a large number of ideal, symmetric, elasto-plastic elements connected in parallel with common stiffness but different distribution of yield strengths, with the added capability to incorporate strength deterioration. The generalized-Masing model facilitates a straightforward implementation of a

distributed element model with infinite number of elements, with no requirement to explicitly track the state of each element. It is based on the initial postulation provided by Masing ; if the virgin (backbone) curve for loading is described by the implicit relationship $f(F, \delta) = 0$, then according to Masing's hypothesis, each branch of the hysteresis loop between points $(-F_a, -\delta_a)$ and (F_a, δ_a) is given by $f(\frac{F - F^*}{2}, \frac{\delta - \delta^*}{2}) = 0$, where (F^*, δ^*) is the load reversal point for the branch, which is $(F^*, \delta^*) = (-F_a, -\delta_a)$ for the loading branch and $(F^*, \delta^*) = (F_a, \delta_a)$ for the unloading branch. The generalized Masing model follows the additional rules (Vetter et al., 2012)

- *Incomplete loops:* The equation of any hysteretic force - drift curve can be obtained by applying the original Masing rule to the virgin curve using the latest point of load reversal. For example, if the virgin loading curve OA in Figure 3.3 is defined by $f(F, \delta) = 0$ then the branch curve CD is defined by $f(\frac{F - F^*}{2}, \frac{\delta - \delta^*}{2}) = 0$ with $(F^*, \delta^*) = (F_c, \delta_c)$.
- *Completed loops:* Once an interior curve crosses a curve from a previous load cycle under continued loading or unloading, a hysteresis loop is completed and the load deformation curve of the previous cycle is continued. For example if the unloading curve in Figure 3.3 is continued to point C, further unloading will follow a path that is extension of the curve ABC.

For completely characterizing the generalized Masing model, the initial stiffness k_i , the maximum force F_u and a parameter n defining the elastic to plastic transition are required.

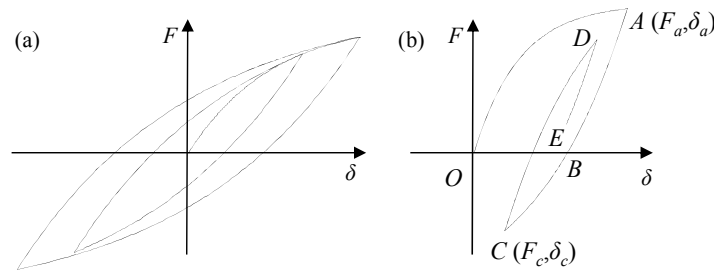


Figure 3.3. Masing model; force-displacement cycles for (a) stable cycle loading and (b) transient loading

3.3. Calibration of parsimonious model

For the calibration of the parsimonious hysteretic models two basic steps are introduced: (i) determination of the linear characteristics and (ii) selection of the remaining characteristics of the backbone curve, with an additional third step corresponding to the evaluation of the fit of the hysteretic behavior between the different available models.

Linear characteristics: If k_i^i denotes the initial stiffness for the restoring force of the i^{th} story then the initial stiffness matrix is $\mathbf{K}_s = \mathbf{T}_s^T [\text{diag}(k_1^1 \dots k_i^i \dots k_n^n)] \mathbf{T}_s$, where $\text{diag}(\cdot)$ denotes a diagonal matrix with diagonal entries the arguments inside the parenthesis. The n -stiffness parameters $\{k_i^i; i = 1, \dots, n\}$ can be then selected to match the fundamental period (1 objective) and modeshape ($n-1$ additional objectives, leading to a total of n -objectives) of the high fidelity structural model. This corresponds to a well-posed system of n nonlinear equations with n unknowns. Through this approach the parsimonious model will have the same linear behaviour as the fundamental mode of the high fidelity structural system.

Backbone characteristics: The characteristics for the backbone curve of each story of the high-fidelity structural model may be obtained through a cyclic pushover analysis. The loading in this analysis (Figure 3.4) corresponds to roof displacement cycles imposed in positive and negative direction. For each floor the restoring force can be then calculated by summing the shear forces of the columns of each floor. Retaining then the history of restoring force - interstory drift of each floor at the displacement reversal instances leads to points approximating the backbone curve of the structural model. For obtaining good resolution the displacement loading pattern needs to gradually increase up to the maximum imposed roof displacement as is depicted in Figure 3.4(a). The characteristics of the

backbone curve for the parsimonious hysteretic model may be then obtained to fit these points. For a piece-wise linear model the number of linear segments needs to be additionally decided, i.e. number of springs connected in parallel, along with the characteristics of each of these segments. For a Masing model the inclusion or not of a strain hardening segment needs to be additionally considered, i.e., addition of a linear spring connected in parallel. Figure 3.4(b) illustrates this fit within the context of the illustrative example considered later for both a piecewise linear model and a generalized Masing model. The details shown in the figure correspond to the first story of the structure and Δ , H and h_i denote the roof displacement, the total building height and the story height, respectively.

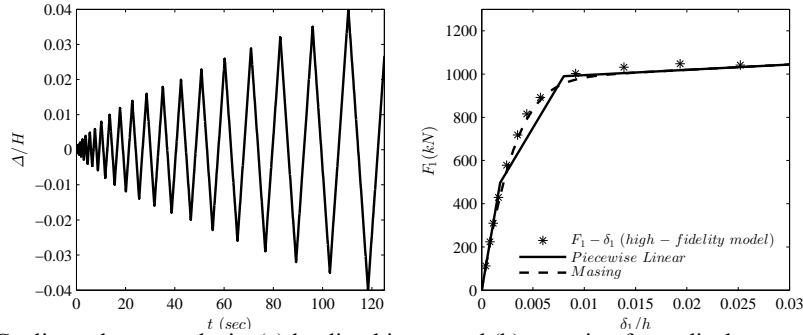


Figure 3.4. Cyclic pushover analysis: (a) loading history and (b) restoring force-displacement points at the instances of load reversal along with the approximations by piecewise linear and Masing backbone curves

Evaluation of fit of hysteresis: The fit of the different hysteretic models is finally evaluated through a sinusoidal loading, possibly with modulated amplitude and frequency to capture the important range of structural dynamics (frequency as well as amplitude of nonlinear vibration). This provides the restoring force – interstory drift time history loop (as shown in Figure 3.5), where the restoring force for the high-fidelity model is obtained in a similar way as for the cyclic pushover case. The different parsimonious hysteretic models (with characteristics determined in the previous two calibration steps) can be then compared to this loop to evaluate which one provides a better fit. The one with the better fit should be then chosen as the parsimonious model providing the best approximation to the nonlinear behavior of the high-fidelity structure. Figure 3.5 illustrates this process for the same case as the example shown in Figure 3.4. It is evident in this case that the peak-oriented model provides a better fit and it is the one that should be preferred.

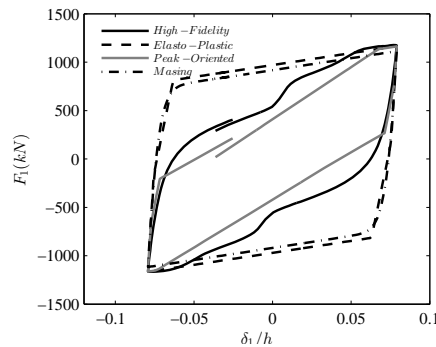


Figure 3.5. Comparison of hysteresis loops from the structural model against the parsimonious hysteretic model

3.4. SIMULINK Implementation

SIMULINK, is a software package, tightly integrated with MATLAB, used for modeling, analyzing and simulating dynamical systems (Klee, 2007). It provides a graphical user interface for constructing the models, using standard block diagram representation, and a wide range of algorithms for simulating their response. An extensive library of standard components is available within SIMULINK (such as integrators, summing junctions, state space representations, saturation, and so forth) whereas additional block sets exist that extend the capabilities of SIMULINK for many diverse

areas of engineering and sciences. After the block diagram of the structural model has been created, any of the available numerical integration routines can be implemented to simulate its response (for any given excitation). The user has the option to select a specific solver and step size (applicable for fixed-step size integration algorithms), or tolerances for satisfying convergence/accuracy requirements.

4. ILLUSTRATIVE EXAMPLE

We now illustrate the concepts discussed in this paper through an example which examines the accuracy and the computational savings of this parsimonious modeling approach by comparison to a high-fidelity structural model (developed in this study in OpenSees (McKenna, 2011)) over an ensemble of 25 ground motion records with different characteristics (leading to different levels of nonlinear behavior). A three story concrete benchmark structure is used for the case study and the comparison is established in terms of interstory drifts responses.

4.1. High fidelity model

The structure considered corresponds to a three-story moment resisting frame office building designed to comply with ASCE-05. The building is designed for a site located in the Los Angeles Basin, which was selected to represent a typical urban high seismic region of California. The structural layout of the building represents a symmetric three-bay by five bay plan with 6.5 m span lengths. The lateral system consists of two exterior moment resisting frames in each direction. The column element sizes are 50x50 cm, 45x45 cm and 40x40 cm for the first, second and third story, respectively, while the beam size is 30x60 cm. For the analysis a two – dimensional model of a three bay frame is created in OpenSees. A fiber model is used to simulate beams and columns. The material stress – strain response in each fiber is integrated to get the stress resultant forces. The nonlinear hysteretic behavior of the element depends in the constitutive material relationship of the concrete and reinforcing steel fibers into which each section is divided. 5% percent Rayleigh damping based on initial stiffness characteristics is included to the structural model. The masses of each floor are found to be 97.52, 95.92 and 92.30 metric tons for the first, second and third floor, respectively.

4.2. Calibration of parsimonious model

The first step for the calibration of the parsimonious model is determination of the linear characteristics following the procedure described in section 3.3; The initial stiffness characteristics of the parsimonious model are selected to match the fundamental mode of the high-fidelity model, which has period of 0.59 sec and modeshape $[\varphi_1^i] = [0.269 \ 0.685 \ 1.000]$, normalized to have value equal to one at top floor. The floor stiffness's for the structure are then found to be $[k_f^i] = [78.9 \ 42.8 \ 33.0]$ MN/m. The next step needed for the calibration of the parsimonious model is the selection of the remaining characteristics of the backbone curve. As discussed earlier the characteristics for the backbone curve of each story of the high – fidelity structural model are obtained through a cyclic pushover analysis. The loading history that was used is depicted in Figure 3.1(a), while Figure 3.4(b) illustrates how the backbone curve of a piecewise linear model and a generalized Masing model of the restoring force – interstorey drift relationship were fitted to the backbone characteristics of the high – fidelity structural model. For the Masing model strain hardening was additionally used by combining in parallel with a linear spring, whereas for the piece-wise linear model a combination of three different nonlinear springs was selected for each floor as it provided a better overall fit to the backbone curve of the hysteretic model. Table 4.1 shows the characteristics of these springs. The last step of the calibration procedure involves the evaluation of fit of the hysteresis loops of the parsimonious hysteretic models to the one obtained by the high fidelity model. The dynamic loading that was used is a sinusoidal time history which was modulated both in amplitude and frequency. The amplitude of the sinusoidal signal was modulated from 0 to 0.4 g, while the frequency was modulated from 2.5 Hz to 0.5 Hz. Figure 3.5 presented earlier illustrates the comparison of the hysteretic loops from the high – fidelity structural model against the three parsimonious hysteretic models.

Table 4.1. Characteristics of springs used for the parsimonious model. Characteristics for all floors are provided in brackets

Characteristic	Piece-wise linear						Characteristic	Masing					
	Spring 1			Spring 2				Spring 3					
k_l (MN/m)	[64.9	28.5	21.8] ^T	[13.4	13.2	10.8] ^T	[0.61	1.14	0.38] ^T	k_l (MN/m)	[78.3	42.2	32.7] ^T
δ_{y+} (cm)	[0.91	1.23	1.05] ^T	[3.50	3.50	4.20] ^T	[28.0	19.3	17.5] ^T	n	[1.4	1.5	1.5] ^T
δ_{y-} (cm)	[0.91	1.23	1.05] ^T	[3.50	3.50	4.20] ^T	[28.0	19.3	17.5] ^T	F_u (kN)	[970	880	640] ^T
									k_l spring in parallel (MN/m)	[0.63	0.64	0.33] ^T	

4.3. Comparison of accuracy and efficiency of parsimonious modeling

This section examines in detail the accuracy and efficiency of the parsimonious modeling approach using the selected ensemble of ground motions. Three different parsimonious models are considered and the notation used is the following:

Masing: Generalized Masing model with an additional strain hardening component.

Elasto-plastic: Piece-wise linear model from combination of three springs with ideal elastic - plastic hysteretic behavior.

Peak-oriented: Piece-wise linear model from combination of three springs with peak-oriented hysteretic behavior.

The restoring force – interstorey drift diagram of the first and the third floor obtained by the high – fidelity structural model and the predicted ones by the parsimonious models for the case of the Kobe earthquake excitation is shown in Figure 4.1. A comparison between the high – fidelity and the parsimonious hysteretic curves reveals very similar qualitative behavior. It is concluded that in general all the three parsimonious models capture most of the important features of the hysteretic behavior of the high – fidelity structural model. It should be noted that the peak oriented hysteretic model provides the best approximation between the three parsimonious models, since it captures also the change of stiffness during the reloading branch of the hysteretic curve. This agrees with the arguments made earlier, at the calibration stage of the models.

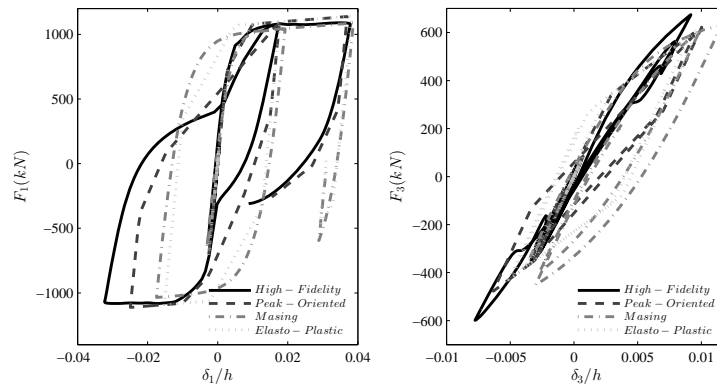


Figure 4.1. Comparison between the high fidelity and the parsimonious restoring force – interstorey drift hysteretic curves of the first (left) and the third floor (right) for the Kobe earthquake record.

The accuracy of the three different parsimonious models is now assessed for the entire ensemble of ground motions by calculation of the average relative absolute error and the coefficient of determination of the maximum responses of the interstorey drift of each floor. These quantities are statistical measures which quantify how good is on average the approximation of a response quantity

compared to the corresponding response of the high fidelity model. The relative absolute error AE is defined as:

$$AE = \frac{\sum_{i=1}^N |v_i - v_i'|}{\sum_{i=1}^N v_i} \quad (2.1)$$

where v_i is the maximum drift response of the high fidelity model for each one of the 25 selected ground motions, v_i' is the corresponding maximum response of the parsimonious model for each one of the 25 selected ground motions, and N is the number of the samples (i.e. the number of the selected ground motions). The relative absolute error quantifies the discrepancy between the assumed “exact” value of the maximum response, obtained by the high-fidelity structural model, and the corresponding approximation predicted by the parsimonious model. The coefficient of determination R^2 is defined as:

$$R^2 = 1 - \frac{\frac{1}{N} \sum_{i=1}^N (v_i - v_i')^2}{\frac{1}{N} \sum_{i=1}^N \left(v_i - \frac{1}{N} \sum_{i=1}^N v_i \right)^2} \quad (2.2)$$

and denotes the proportion of variation in the data that is explained by the parsimonious model. Smaller values for the absolute error correspond to more reliable predictions for the approximate (i.e. parsimonious) model. Values for the coefficient of determination close to 1 indicate that the parsimonious model can adequately capture the variability of the high-fidelity responses.

Table 3 show the relative absolute error and the coefficient of determination calculated for the three different parsimonious models for the maximum interstorey drift of each floor. In general, the quality of approximation obtained by the parsimonious modeling approach is satisfactory, since the relative absolute error varies approximately from 7% to 13.5% and the coefficient of determination varies from 0.90 to 0.99. It is important to note that comparisons (Aviram et al., 2008) between different high-fidelity models for non-linear structural behavior (established with different modeling assumptions for addressing the nonlinear structural behavior) yield similar levels of errors in peak responses. As such the accuracy established in the current study should be considered as good.

Table 4.2. Relative absolute error and coefficient of determination of the maximum interstorey drift of the three parsimonious models

Model	AE (%)			R		
	1 st Floor	2 nd Floor	3 rd Floor	1 st Floor	2 nd Floor	3 rd Floor
Peak - Oriented	9.61	7.27	11.65	0.99	0.98	0.93
Masing	11.86	10.29	10.92	0.99	0.99	0.95
Elasto - Plastic	12.31	10.71	13.47	0.99	0.98	0.90

Assessing, now, the quality of the approximation obtained from the three different parsimonious models that were used, it is evident that the peak oriented hysteretic model provides the most reliable approximation in terms of interstorey drifts. This agrees with the comments made earlier, and provides tangible validation of the proposed third step in the calibration process for choosing the most appropriate parsimonious model. It is noted that the quality of approximation deteriorates for the response quantities of the third floor whereas the third floor’s response is significantly less non-linear than the response of the other two floors (see Figure 4.2 later). The former behavior in conjunction with the latter observation is attributed to the fact that the third floor is more sensitive to higher mode effects and that the calibration of the linear characteristics of the parsimonious model was established by matching only the fundamental natural period and modeshape of the high – fidelity structural model. It should be noted that the high value of the coefficient of determination, especially for the peak-oriented and Masing models, show that the parsimonious modeling approach captures very well the variability of the response for the ensemble of earthquakes. This characteristic is of particular importance for seismic risk estimation. As discussed in the introduction, this estimation requires

evaluation of structural response for a large number of earthquake scenarios and it is more important to depict the overall variability correctly, rather than having small errors on scenario-by-scenario basis.

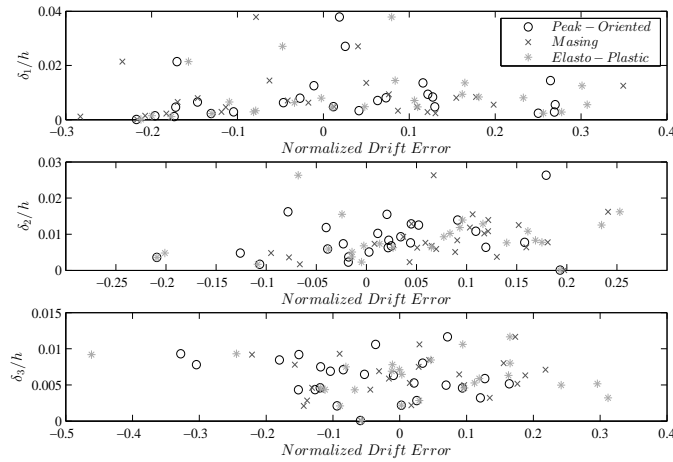


Figure 4.2. Normalized error for the maximum interstory drift response versus the maximum interstory drift response (obtained by the high – fidelity model)

Figure 4.2 further shows the variation of the error between the corresponding maximum response drift of the high-fidelity model and the parsimonious model normalized by the respective response of the high-fidelity model versus that response, for each one of the selected ground motion records (sample plots). The y-axis in these figures corresponds to different levels of nonlinear response. As such the figures further allow for comparison of the errors established for different nonlinear response levels as well as identification of potential correlations. These figures indicate that the parsimonious modeling approach captures adequately well the global maximum response characteristics, since the individual errors are in general less than 25% for the interstory drift of the first two floors, with most excitations providing significantly smaller errors. Again a deterioration of the approximation for the responses of the third floor is verified, whereas the drifts in this floor are significantly smaller indicating smaller level of nonlinear behavior. The maximum individual errors range between 25% to 35%. Comparing the three parsimonious models, it is verified that the peak oriented model provides better approximation. Additionally there is no bias evident regarding the interstory drift of all the floors. The absence of any evident bias is another indication of the adequate accuracy achieved with the parsimonious modeling approach. Finally it should be pointed out that the figure indicates no correlation between having bigger errors with higher (or lower) response values; this correlation is judged by comparing the x-y axis distribution of the samples in the different plots. This further validates the accuracy of the parsimonious model for different regions of nonlinear response.

Table 4.3. Comparison of average computational time per earthquake between the high fidelity model and the parsimonious models

Model	Computational time (sec)	computational time of parsimonious model	
		computational time of high fidelity model	
High - fidelity	671.2	1.0	
Peak - oriented	0.25	$3.7 \cdot 10^{-4}$	
Masing	0.17	$2.5 \cdot 10^{-4}$	
Elasto - plastic	0.30	$4.5 \cdot 10^{-4}$	

Finally for evaluating the computational efficiency of the parsimonious modeling approach, Table 4.3 presents the average computational time per earthquake for the high fidelity model simulated in OpenSees and the parsimonious models. It is mentioned that in OpenSees the standard numerical time integration scheme used is the two parameter time-stepping method developed by Newmark, whereas in SIMULINK the fixed step Bogacki-Shampine solver algorithm was used. The time step used for

both cases was equal to 0.01 sec. The great computational savings achieved of all the parsimonious models are obvious, since they turned to be up to 3948 times more efficient than the high – fidelity model at the expense of relatively small reduction in accuracy, as discussed earlier.

5. CONCLUSIONS

A parsimonious modeling approach for the hysteretic behavior of nonlinear structures utilizing the versatile SIMULINK modeling environment in MATLAB was discussed in this paper. The parsimonious models are established by globally describing the restoring force – interstory drift hysteretic relationship of each floor through introduction of nonlinear spring elements. Three different models for this hysteretic behavior were examined in the current study, and detailed discussion pertaining to their calibration using information from high-fidelity structural models was presented. In the proposed approach the linear properties of the parsimonious models are selected to match the fundamental structural mode, whereas the remaining characteristics of the hysteretic backbone behavior are chosen based on the behavior of the high-fidelity model under cyclic pushover analysis. The different parsimonious hysteretic models are finally evaluated by comparison to the response of the high fidelity model under sinusoidal loading, and the one providing the overall best fit is finally chosen. An illustrative example was presented for which the high-fidelity structural model was developed in the versatile OpenSees structural analysis software. The calibration steps were demonstrated and finally the accuracy of the parsimonious models was evaluated over a large ensemble of ground motion records by comparing to the results obtained from the high fidelity model. The results show that the parsimonious modeling within the SIMULINK environment offers great computational savings and provides results with good accuracy compared to the high fidelity predictions, which can additionally very well capture the variability of the response over the set of ground motion records considered. The latter is a very important result, since in seismic risk assessment we are primarily interested of adequately describing the response and its variability over a large number of excitation scenarios, rather than accurately describing that behavior for specific excitations. The peak oriented model was predicted in the calibration stage to provide a better fit to the high fidelity model and this was verified in the evaluation over the suite of excitations considered; it provided small average errors and very high accuracy in describing the variability of the seismic response. The Masing model also provided adequate accuracy results. Overall the study proved the efficiency of the proposed parsimonious modeling approach as well as of the calibration process proposed, and the computational advantages when this modeling framework implemented within the SIMULINK environment.

REFERENCES

- Aviram, A., Mackie, K. R. & Stojadinovic, B. (2008). Guidelines for Nonlinear Analysis of Bridge Structures in California. *PEER Technical Report 2008/03*.
- Bertero, V. V., Mahin, S. A. & Herrera, R. A. (1978). Aseismic design implications of near-fault San-Fernando earthquake records. *Earthquake Engineering & Structural Dynamics*, **6**, 31-42.
- Klee, H. (2007). Simulation of dynamic systems with MATLAB and SIMULINK, Boca Raton, FL, CRC Press.
- Mckenna, F. (2011). OpenSees: A Framework for Earthquake Engineering Simulation. *Computing in Science & Engineering*, **13**, 58-66.
- Spacone, E., Filippou, F. C. & Taucer, F. F. (1996a). Fibre beam-column model for non-linear analysis of R/C frames .1. Formulation. *Earthquake Engineering & Structural Dynamics*, **25**, 711-725.
- Spacone, E., Filippou, F. C. & Taucer, F. F. (1996b). Fibre beam-column model for non-linear analysis of R/C frames .2. Applications. *Earthquake Engineering & Structural Dynamics*, **25**, 727-742.
- Taflanidis, A. A. & Beck, J. L. (2009). Life-cycle cost optimal design of passive dissipative devices *Structural Safety*, **31**, 508-522.
- Vetter, C., Gidaris, I. & Taflanidis, A. A. (Year). Seismic hazard characterization through stochastic ground motion modeling. *In: ASCE 2012 Structures Congress, 2012 Chicago, Illinois*.